

# Birefringent Fresnel Zone Plates in Silica by Femtosecond Laser Machining

Erica Bricchi, John D. Mills, Peter G. Kazansky, and

Bruce G. Klappauf

Optoelectronics Research Centre,

University of Southampton, Southampton SO17 1BJ, UK

*erb@orc.soton.ac.uk*

Jeremy J. Baumberg

Department of Physics and Astronomy,

University of Southampton, Southampton SO17 1BJ, UK

We demonstrate maskless, single-step fabrication of strongly birefringent Fresnel zone plates by the focusing of femtosecond laser pulses deep within silica substrates. The process allows alternate zone rings to be directly produced within the substrate by inducing a local refractive index modification of the order  $n \sim 10^{-2}$ . The embedded zone plates shown in this letter present efficiencies that vary by a factor of up to  $\sim 6$  for orthogonal polarizations. Focal lengths of primary and secondary foci are shown to compare well with theory. ©2002 Optical Society of America

**OCIS codes:** (140.3390) Laser material processing; (130.1750) Components

Fresnel zone plates are attractive devices for micro-optics due to their focusing abilities and compactness.<sup>1</sup> However, methods of fabrication are usually based on either lithographic<sup>2,3</sup> or etching techniques.<sup>4</sup> In this letter, we report a system for producing zone plates by using a focused femtosecond laser to machine individual zone rings within the bulk of silica. The process offers enormous advantages over current zone plate fabrication since it is a one-step procedure and holds the potential for creating polarization-sensitive, integrated multi-lens systems in three-dimensions. Indeed the microfabrication of structures within the bulk of transparent materials with focused femtosecond laser pulses has become of more interest in recent years.<sup>5,6</sup> Within the focal volume, nonlinear absorption causes energy to be deposited that induces a permanent refractive index modification.<sup>7</sup> By translating a sample relative to the focus of the laser, a variety of photonic devices have already been created.<sup>8,9</sup> Using the facility of index manipulation, the femtosecond direct-write procedure is well-

suited to create the phase variations necessary for efficient Fresnel zone plate production. Figure shows the experimental set-up for the single-step lens fabrication. A regeneratively-amplified, mode-locked Ti:Sapphire laser operating at wavelength  $\lambda = 850$  nm with 150 fs pulse duration and 250 kHz repetition rate, was utilized to effect the direct-write process. Its collimated beam passed through an electronic shutter, variable neutral density filter and half-wave plate before a dichroic mirror reflecting only in the 400-700 nm region. The laser light traveled through the mirror and was focused to beam-waist diameter of  $\sim 1.5 \mu\text{m}$  via a 50x (NA = 0.55) objective into a fused silica plate at a depth of about 0.5 mm. The sample was mounted upon a computer controlled linear motor translation stage of 20 nm resolution in all three dimensions. To simultaneously observe the zone plate writing process, a white-light illuminating source enabled the structure to be monitored by a charge-coupled device camera via suitable filters.

A Fresnel zone plate consists of a series of concentric rings, whose outer radius  $R_m$  is determined by

$$R_m = \sqrt{mfl} \quad (1)$$

where  $m$  is the number of the  $m$ th-Fresnel zone,  $\lambda$  the wavelength in vacuum and  $f$  the primary focal length.<sup>10</sup> Figure 2 shows a microscope image of the central region of a Fresnel zone plate (Lens A) created by the direct-write method. The image, acquired by positioning the lens between cross-polarizers, demonstrates the strong birefringence of this directly-written structure. The particular lens has a maximum radius of 1 mm, 70 zones and is designed to focus light with wavelength  $\lambda = 632.8$  nm at a length of 2.4 cm. The writing energy was  $1.3 \mu\text{J}/\text{pulse}$ . In order to produce the quasi-uniform regions of index variation

in odd-numbered zones, the sample was translated in circles of ever-increasing radius at a constant speed of 400  $\mu\text{m/s}$ . Even-numbered zones were not touched.

In addition to a primary focus, Fresnel zones plates present a series of secondary foci displaced on an axis towards the lens that are characterized by a much weaker intensity.<sup>11</sup> In order to measure the positions of these foci in the case of directly-written zone-plates, a further sample (Lens B) was examined. This particular lens was written with a slightly lower energy to that of Lens A at 1.1  $\mu\text{J/pulse}$ , but at the equivalent writing speed of 400  $\mu\text{m/s}$ . It has a maximum radius of 1 mm, 158 Fresnel zone plates and is designed to focus light with wavelength 632.8 nm at a length of 1 cm. To enable the positions of its primary and secondary foci to be recorded, a white-light source was directed through various transmission interference filters in turn, before becoming incident on the zone plate itself. A CCD camera mounted upon a translation stage was subsequently placed behind the zone plate such that it could be moved along its axis to identify the positions of its foci. Effective focal positions were examined for wavelengths 488 nm, 550 nm and 642 nm. The results are displayed in Figure 3, where focal positions (points) are compared to theory (lines). The theoretical plots given in Figure 3 take into account the dual media of silica and air (see inset in Figure 3) and are calculated from the standard Eq. (1):

$$f = \frac{f_1 \lambda_1}{\lambda} \quad (2)$$

where  $f_1$  and  $\lambda_1$  are the value of the focal length and wavelength used in Eq. (1) to fabricate the Fresnel zone plate,  $\lambda$  is the wavelength of interrogating light and  $f$  its particular focal length. As can be seen, the experimental results are within 1% of theory for all wavelengths, primary and secondary foci. However, theory only predicts a series of odd secondary foci

at  $f/3$ ,  $f/5$  etc,<sup>11</sup> but in the case of Lens B, there are identifiable even secondary foci at  $f/2$  and  $f/4$ . This anomaly can be explained in terms of the Fresnel zones having slightly unequal areas.<sup>11</sup> In the case of the directly-written zone plates described here, is due to the writing resolution, which for our set up is  $\sim 1.5\mu\text{m}$ . In order to demonstrate the focusing quality of a directly-written Fresnel zone plate, Figure 4 shows an image of the Southampton University logo produced by Lens B. The logo was illuminated with a white-light source and imaged through the zone plate. An interference filter and a polarizer were positioned before the lens, and the focal plane was recorded via a charge-coupled device camera. The object size at  $\sim 4\text{mm}$  diameter can be compared to the image size in the focal plane of  $\sim 600\mu\text{m}$  diameter.

The technique of femtosecond direct-writing in silica has been observed to create birefringent structures in silica above a certain threshold of writing-fluence.<sup>12,13</sup> We have recently published experimental evidence of the primary cause of this anisotropic behavior, which occurs at a threshold of  $\sim 0.5\mu\text{J}/\text{pulse}$  using the present experimental set-up.<sup>14</sup> It follows that different polarizations of light incident on a Fresnel zone plate created above this threshold, will “see” different refractive indexes and therefore phase as the light passes through the directly-written regions. Indeed, with much higher writing fluence as in the case of Lenses A and B, strongly birefringent zone-plates can be created with efficiencies that vary by a factor of up to  $\sim 6$  for orthogonal polarizations. These lenses therefore show the interesting property of having a selective ability to focus orthogonal polarizations of incident light independently, which may be useful for integrated optical circuits or Micro-Electro-Mechanical-Systems applications that require both focusing and polarization sensitive properties.

Table 1 elucidates these properties by showing a range of efficiencies calculated as a function of wavelength and polarization for Lenses A and B. The direction of polarization of the interrogating light is either parallel to the direct-write laser polarization ( $xx$ ) or perpendicular to the direct-write laser polarization ( $xy$ ). The efficiency was derived as the ratio of power in each primary focus and total power incident on the zone plates.

It is interesting to note by examination of Table 1 that a wide range of efficiencies for Lenses A and B are produced for the variety of wavelengths and polarizations tested. This is due to the varying degrees of constructive/destructive interference due to the phase variations induced by the index-modified zones.<sup>10</sup> As known, zone plates that focus as a function of a phase variation induced in alternate zones have a theoretical maximum efficiency of approximately 40% assuming a variation of  $\pi$  and 100% transmission through the lens. This can be compared to absorbing zone plates that have a maximum efficiency of just 10%.<sup>15</sup> With a maximum efficiency recorded of 39%, our results therefore indicate that the direct-written zone plates behave as phase lenses. In order to estimate the phase variation produced by the particular writing parameters described here, two methods of characterization were used. Firstly, embedded diffraction gratings directly-written into the bulk of a silica plate under similar writing conditions to Lens B, were subsequently tested by examining the diffracting orders of a HeNe ( $\lambda = 632.8$  nm) laser incident on the gratings, for both  $xx$  and  $xy$  polarizations. Numerical methods were then initiated to simulate the results using Fresnel-Kirchoff diffraction theory. From this procedure, estimated index variations at the modified regions of  $\Delta n \sim 2 \times 10^{-3}$  ( $xy$ ) and  $\Delta n \sim 9 \times 10^{-3}$  ( $xx$ ) were deduced. Secondly, the recorded efficiencies given in Table 1 were utilized to estimate the refractive index from the thickness and transmission coefficient of the zone plates by using the integrals described by Kirz.<sup>10</sup> These

values were then averaged to give estimated index variations of  $\Delta n \sim (2, 3) \times 10^{-3}$  ( $xy$ ) and  $\Delta n \sim (5, 6.5) \times 10^{-3}$  ( $xx$ ), where the greater value corresponds to the higher writing-fluence in each case. The phase variation between the silica (untouched) zones and the femtosecond modified zones was subsequently estimated from the latter method to be  $\sim 0.2 \pi$ ,  $\sim 0.3\pi$  ( $xy$ ) and  $\sim 0.5 \pi$ ,  $\sim 0.6\pi$  ( $xx$ ) respectively, for an interrogating wavelength of 632.8 nm. Indeed, the high efficiencies described in Table 1 indicate that phase variations between alternate zones of  $\sim \pi$  can easily be achieved for particular wavelengths. This is interesting because full-range controllability of phase across these directly-written embedded objects offers the possibility of manufacturing other optical components such as embedded wave-plates. In the light of these results, we are working to optimize the parameters of our direct-write process to afford greater controllability over device fabrication for particular design wavelengths.

In summary, we have demonstrated the single-step production of strongly birefringent, embedded Fresnel zone plates by femtosecond laser direct-machining. The process offers potential for polarization-sensitive, integrated multi-lens systems. We are currently working to maximize the potential of the anisotropic zone plates for individual design wavelengths.

## References

1. N. Kitaura, S. Ogata, and Y. Mori, *Opt. Eng.* **34**, 584 (1995).
2. L. Mingtao, J. Wang, L. Zhuang, and S. Y. Chou, *Appl. Phys. Lett.* **76**, 673 (2000).
3. M. Haruna, M. Takahashi, K. Wakahayashi, and H. Nishihara, *Appl. Opt.* **29**, 5120 (1990).
4. J. Canning, K. Sommer, S. Huntington, and A. Carter, *Opt. Comm.* **199**, 375 (2001).
5. K. Miura, J. Qiu, H. Inouye, T. Mitsuyu, and K. Hirao, *Appl. Phys. Lett* **71**, 3329 (1997).
6. M. D. Berry, B. C. Stuart, P. S. Banks, M. D. Feit, V. Yanovsky, and A. M. Rubenchik, *J. Appl. Phys.* **85**, 6803 (1997).
7. E. N. Glezer and E. Mazur, *Appl. Phys. Lett.* **85**, 6803 (1997).
8. K. Hirao and K. Miura, *J. Non-Cryst. Solids* **239**, 91 (1998).
9. H. Sun, Y. Xu, S. Juodkazis, K. Sun, M. Watanabe, S. Matsuo, H. Misawa, and J. Nishii, *Opt. Lett.* **26**, 325 (2001).
10. J. Kirz, *J. Opt. Soc. Am.* **64**, 301 (1974).
11. J. Higbie, *Am. J. Phys.* **44**, 929 (1976).



12. L. Sudrie, M. Franco, B. Prade, and A. Mysyrowicz, *Opt. Commun.* **171**, 279 (1999).
13. P. G. Kazansky, H. Inouye, T. Mitsuyu, K. Miura, J. Oiu, and K. Hirao, *Phys. Rev. Lett.* **82**, 199 (1999).
14. J. D. Mills, P. G. Kazansky, E. Bricchi, and J. J. Baumberg, *Appl. Phys. Lett.* (to be published).
15. H. Nishihara and T. Suhara, "Principles of Fresnel Lenses" in *Progress in Optics* (Elsevier Science Publishers B. V. Amsterdam, 1987), Vol. 24, pp. 5–11.

## List of Figures

Fig. 1. Experimental set-up for the single-step fabrication.

Fig. 2. Microscope image of the central part of a femtosecond direct-written Fresnel zone plate positioned between cross-polarizers.

Fig. 3. Measured focal lengths (points) and theoretical focal lengths (lines) of Lens B.

Fig. 4. Image of the Southampton University logo produced by an embedded Fresnel lens.

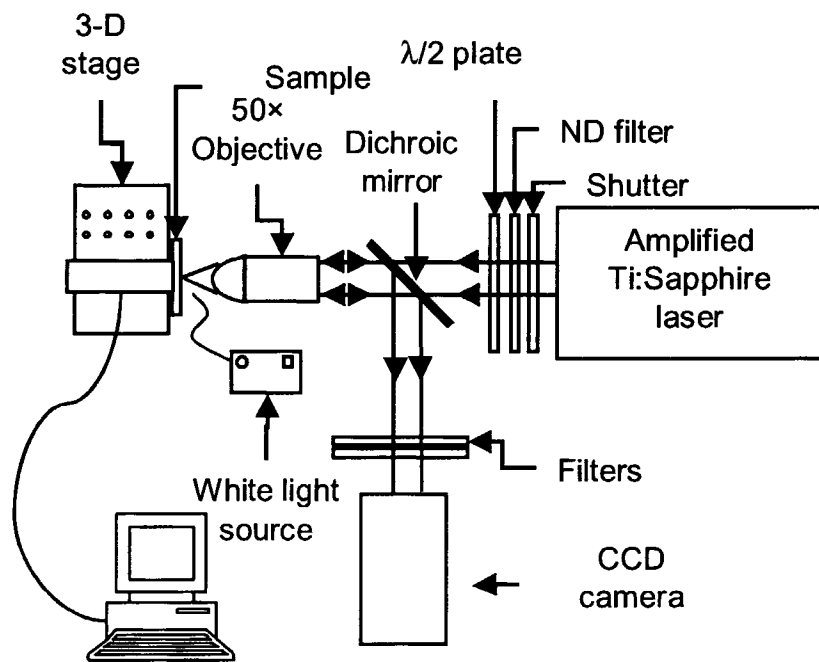


Figure , E. Bricchi et. al.

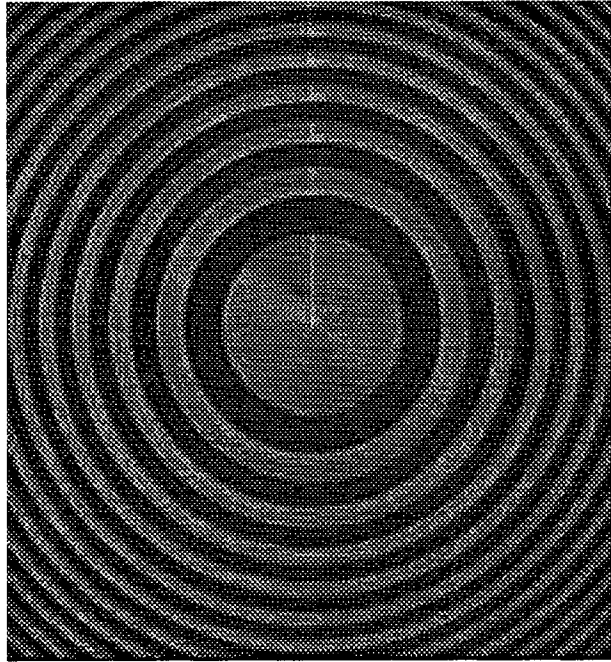


Figure 2, E. Bricchi et. al.

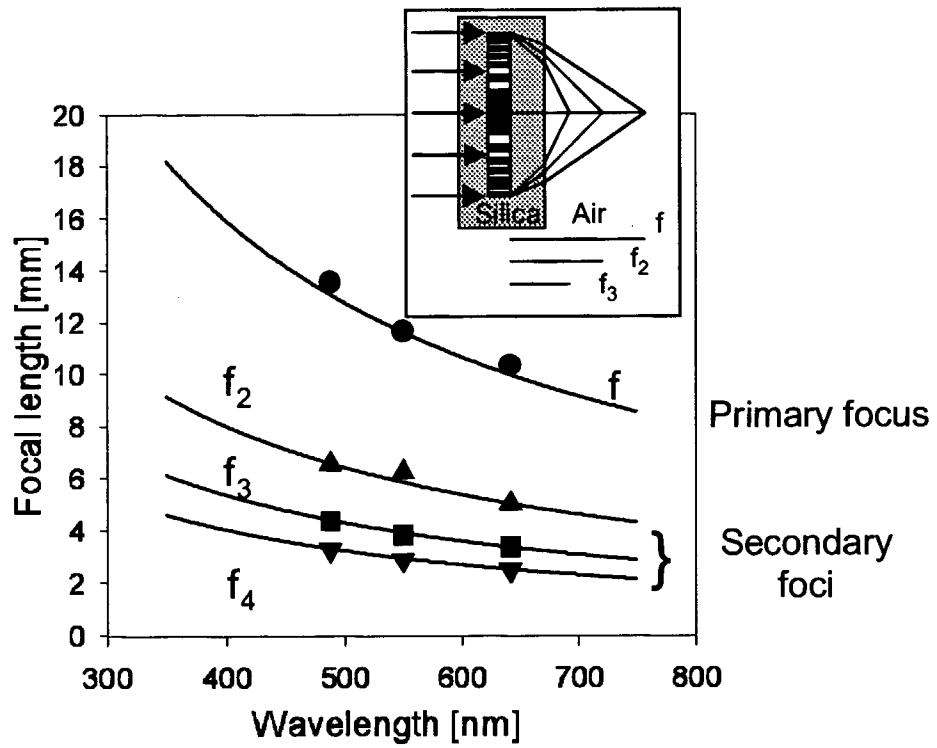


Figure 3, E. Bricchi et. al.

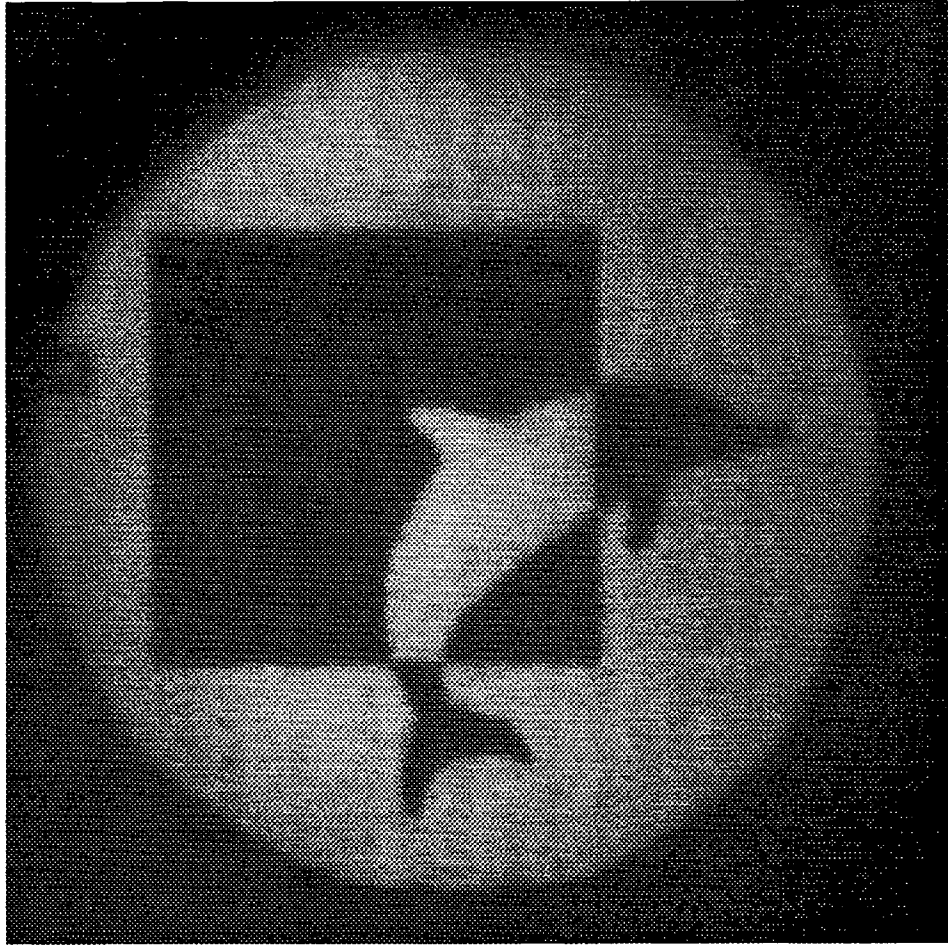


Figure 4, E. Bricchi et. al.

Table 1. Experimental results on efficiency and index modification of Lenses A and B for given interrogating wavelengths and polarization.

Lens	$\lambda$ [nm]	Polarization	Efficiency [%]	Index modification [ $\times 10^{-3}$ ]
A	404	<i>xx</i>	39	6.2
A	404	<i>xy</i>	11	2.4
A	550	<i>xx</i>	34	6.9
A	550	<i>xy</i>	10	3.1
A	642	<i>xx</i>	26	6.4
A	642	<i>xy</i>	9	3.4
B	404	<i>xx</i>	28	4.3
B	404	<i>xy</i>	7	1.9
B	550	<i>xx</i>	24	5.2
B	550	<i>xy</i>	4	1.9
B	642	<i>xx</i>	17	4.9
B	642	<i>xy</i>	3	1.9